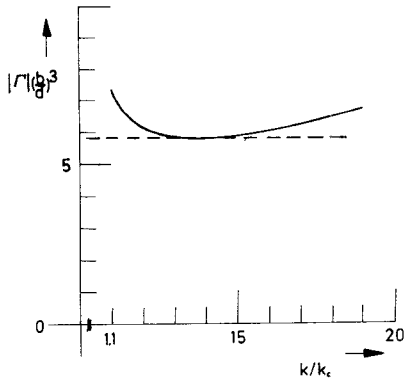

Fig. 8. Reflection coefficient of a sphere on the center of the broad wall in a rectangular waveguide with $b=10.16$ mm and $b/a=0.445$. ——theoretically found behavior as given by (33) - - - - empirically found behavior for small sphere diameters, see [2].

This coefficient, normalized to $(d/b)^3$, versus normalized frequency k/k_c is shown in Fig. 8. It agrees quite well with the small diameter approximation of (1),

$$|\Gamma| = 5.8(d/b)^3 \tag{34}$$

which was found experimentally. Furthermore, the frequency dependence of the reflection coefficient was reported to be within 10 percent of its midband value between $1.22 \leqslant k/k_c \leqslant 1.7$, [2], which is also confirmed by the analytical calculations leading to (33) and Fig. 8.

VI. Conclusions

A method has been shown to calculate the T-section equivalent circuit and the reflection coefficient for a metallic sphere in a rectangular waveguide. Experimental and theoretical results agree quite well. The theoretical method applied here can also be applied to the T-section equivalent circuits for obstacles with other forms in uniform waveguides.

Acknowledgment

The author wishes to acknowledge the hint at the problem and further comments made by P. I. Somlo as well as helpful discussions with P. Gutmann.

References

[1] P. I. Somlo, Talk at Physikalisch-Technische Bundesanstalt, Braunschweig (PTB), July 1978.
[2] ——, "Conductive contacting spheres on the centre of the broad wall of rectangular waveguides," *Electron. Lett.*, vol. 8, no. 20, 1972.
[3] H.-G. Unger, *Elektromagnetische Wellen II*. Braunschweig, Germany: Vieweg, 1967.
[4] ——, *Theorie der Leitungen*. Braunschweig, Germany: Vieweg, 1967.
[5] I. N. Bronstein and K. A. Semendjajew, *Taschenbuch der Mathematik*, 7th ed. Zürich/Frankfurt am Main, Germany: Harri Deutsch, 1967.
[6] S. Chikazumi, *Physics of Magnetism*. New York: Wiley, 1964.

On the Propagation of Leaky Waves in a Longitudinally Slotted Rectangular Waveguide

JAMES M. TRANQUILLA, MEMBER, IEEE, AND J. EUGENE LEWIS, SENIOR MEMBER, IEEE

***Abstract*—The field theory approach is used to study leaky-wave propagation in a rectangular waveguide with long nonresonant slots in the narrow walls. Radiation from the slots is confined by parallel plates which act as transmission lines guiding the energy away from the slots. The complex dispersion equations for TE waves are examined and solved using an iterative numerical technique. Propagation characteristics both in the axial and transverse directions are presented, along with the electric field distribution and power flow. Restrictions on the analysis and on the power-handling capacity imposed by slot width also are described. Measurements of the phase characteristics of the dominant mode are in good agreement with theoretical values.**

Manuscript received May, 1979; revised January 16, 1980. This work was supported by the Natural Sciences and Engineering Research Council of Canada.

The authors are with the Department of Electrical Engineering, University of New Brunswick, P.O. Box 4400, Fredericton, N.B., Canada E3B 5A3.

I. Introduction

SLOTTED WAVEGUIDES are used both as applicators for material processing [1], [2] and as antennas [3]. In particular, traveling-wave slotted structures are used in antenna design [4] because of their ease of construction and their ability to control radiation by varying the slot geometry along the length of the guide.

Typically, the analysis of leaky-wave structures has been carried out using a microwave network representation of the transverse discontinuity [5]. This requires a previous knowledge of the fields which are regarded as weak perturbations of those which would exist in the closed perfectly conducting guide. An alternative approach is to determine the propagation coefficient from the field solution which satisfies the boundary conditions.

0018-9480/80/0700-0714$00.75 ©1980 IEEE

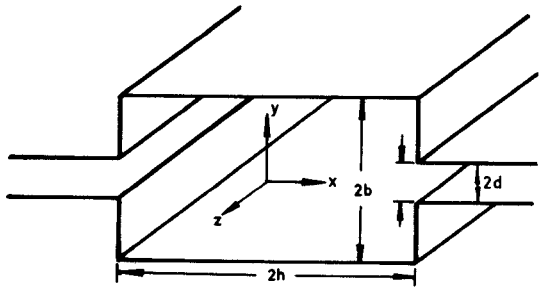

Fig. 1. Geometry of slotted waveguide.

This technique yields a more accurate field representation, although the resulting complex transcendental equation must be solved by an iterative technique using a digital computer.

The geometry of interest, shown in Fig. 1, consists of a rectangular waveguide with long axial slots in both narrow walls feeding parallel plates which enclose lateral regions capable of guiding energy away from the slots. This configuration was first studied by Snurnikova [6], who gave the axial fields and characteristic equations for TE waves. The purpose of this paper is to extend that work. Since both narrow slots and truncated-series field expressions are required in order to solve the characteristic equations, the effects of these approximations on the propagation coefficients and the matching of the boundary conditions are examined. Experimental verification of the axial phase coefficient is reported along with a study of the power-handling capability of the guide. Also, since the development of Snurnikova's characteristic equations has not been reported previously, this is outlined briefly in the Appendix.

II. TE Wave Solutions

Radiation from a continuous longitudinal slot in a lossless uniform waveguide can be described by a fast traveling wave with a complex propagation coefficient [5]. The attenuation of the wave accounts for a continuous leakage of energy. The TE solution [6] can be written

$$H_{z1}=\sum_{n=-\infty}^{\infty} A_n \begin{matrix}\cos\\ \sin\end{matrix}(p_n x)\exp\left(j\frac{n\pi y}{b}\right) \tag{1}$$

$$H_{z2}=\begin{cases}\displaystyle\sum_{r=0}^{\infty} B_r \exp(jq_r x)\cos\left(\frac{r\pi}{2d}\right)(y+d), & x>h\\ \displaystyle\sum_{n=0}^{\infty} B_r \exp(-jq_r x)\cos\left(\frac{\pi r}{2d}\right)(y+d), & x<-h\end{cases} \tag{2}$$

where A_n and B_r are Fourier coefficients n and r are integers, and subscripts 1 and 2 refer to the main waveguide and lateral regions, respectively. The common propagation factor $\exp j(\gamma z-\omega t)$ has been omitted, and the propagation coefficient is defined by

$$\gamma=\beta+j\alpha. \tag{3}$$

The choice of the cosine or sine function in (1) determines the symmetry of the fields about the $x=0$ plane, while the integer r in (2) indicates the order of harmonic y variation of the fields in the lateral regions. The complex wavenumbers p_n and q_r are given by

$$p_n^2=k^2-\gamma^2-\left(\frac{n\pi}{b}\right)^2 \tag{4}$$

$$q_r^2=k^2-\gamma^2-\left(\frac{r\pi}{2d}\right)^2. \tag{5}$$

It will be shown in the following section that the $r=0$ term in (2) is sufficient to describe the fields in the lateral regions. Since $K>\beta$ for fast waves, then from (3) and (5) letting $r=0$ results in q_r having positive real and negative imaginary parts. This corresponds to waves traveling in the lateral regions away from the slots with growing amplitude. This is characteristic of leaky waves; nevertheless, it has been shown [5] that such behavior may provide a valid and highly convergent representation of the field close to the slot.

Choosing the cosine function in (1) corresponds to TE_{mn} modes in the closed waveguide where m is an even integer. Applying Maxwell's equations to find the transverse field components for this case, and matching the appropriate boundary conditions yields the equation

$$A_n+\frac{j}{p_n \sin p_n h}\sum_{s=-\infty}^{\infty} A_s \cos p_s h \sum_{r=0}^{\infty}\Delta_r=0, \qquad n=0,\pm1,\pm2,\cdots \tag{6}$$

where

$$\Delta_r=\frac{2ns\theta^3 q_r \sin[\pi(n\theta-r/2)]\sin[\pi(s\theta-r/2)]}{\pi^2(n^2\theta^2-r^2/4)(s^2\theta^2-r^2/4)} \tag{7}$$

and

$$\theta=d/b. \tag{8}$$

The derivation of (6) is given in the Appendix, while a similar equation exists for the sine function in (1) corresponding to TE_{mn} waves where m is an odd integer

$$A_n-\frac{j}{p_n \cos p_n h}\sum_{s=-\infty}^{\infty} A_s \sin p_s h \sum_{r=0}^{\infty}\Delta_r=0, \qquad n=0,\pm1,\pm2,\cdots. \tag{9}$$

III. TE Wave Solutions for Thin Slots

Equations (6) and (9) can be solved easily only when certain approximations are made. Only the zeroth-order wave ($r=0$) will propagate in the lateral regions if the plates are separated by less than a half wavelength. The ratio of the cutoff frequency of the first-order ($r=1$) wave to that of the dominant TE_{10} mode in the main guide is given by

$$F=h/(b\theta). \tag{10}$$

For standard-ratio guides of $h/b=2$, and for $\theta<0.3$, the cutoff frequency of the $r=1$ wave is sufficiently high that several lower order modes may exist in the main guide without exciting waves with $r>0$ in the lateral regions. Hence it is adequate to employ only the $r=0$ term in (2) if the slots are thin. In this case the axial fields may be

written

$$H_{z1} = \sum_{n=0}^{\infty} A_n \begin{matrix}\cos \\ \sin\end{matrix}(p_n x) \cos\frac{n\pi y}{b} \tag{11}$$

$$H_{z2} = B_0 \exp(jk_c x). \tag{12}$$

The ratio of coefficients A_n/A_0 can be found from (A10) with $r=0$

$$\frac{A_n}{A_0} = \frac{p_0}{p_n} \frac{\sin(n\pi\theta)}{n\pi\theta} \frac{\sin(p_0 h)}{\sin(p_n h)}. \tag{13}$$

Due to the $(\sin n\pi\theta)/n\pi\theta$ factor, higher order terms in n become increasingly insignificant and a truncated series provides a valid field description in the main guide. Following the method given in the Appendix, approximate characteristic equations corresponding to (6) and (9) can be found.

$$1 + 2j\theta K_c h \sum_{n=0}^{\infty} \frac{\cot p_n h}{p_n h} \frac{\sin n\pi\theta^2}{n\pi\theta} = 0, \qquad n = 0, \pm 1, \pm 2, \cdots \tag{14}$$

$$1 - 2j\theta K_c h \sum_{n=0}^{\infty} \frac{\tan p_n h}{p_n h} \frac{\sin n\pi\theta}{n\pi\theta} = 0, \qquad n = 0, \pm 1, \pm 2, \cdots. \tag{15}$$

IV. Propagation Characteristics

The simplified equations (14) and (15) were solved for the complex propagation coefficients of the TE_{10} and TE_{20} waves. A Muller numerical scheme was employed and the series were truncated after twenty terms due to their rapid convergence. The axial phase and attenuation coefficients for several slot widths are shown in Fig. 2 and Fig. 3, respectively. These characteristics show that propagation can occur at frequencies far below the normal cutoff frequencies of the corresponding modes in the closed waveguide. Far above normal cutoff the presence of the slots cause only slight change to the propagation coefficient of the closed waveguide. The attenuation very rapidly decreases with increasing frequency, indicating a diminishing leakage into the lateral regions, and the phase coefficient quickly assumes that of the field in the closed guide. As anticipated, these characteristics are more pronounced for the narrower slots.

The transverse phase coefficient β_t is shown in Fig. 4. The most notable feature of this characteristic is the transition of the field in the lateral regions from a slow to a fast wave in the transverse direction. Provided the slot is narrow, this transition occurs as the frequency is increased through the normal cutoff of the corresponding mode in the closed waveguide.

A number of measurements of the axial phase characteristics were made in standard S- and X-band guides with different slot widths. The normalized wavelengths are shown in Fig. 5 for a frequency range above the normal TE_{10} mode cutoff of the closed guide. The agreement of the measurements with the theoretical results attests to the validity of the approximations made in solving the characteristic equation.

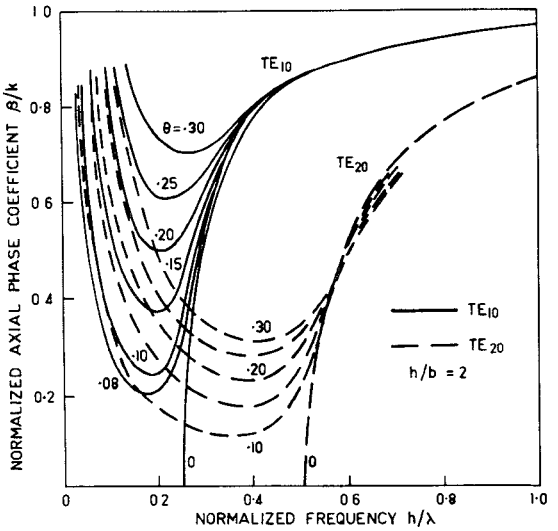

Fig. 2. Normalized axial phase characteristics.

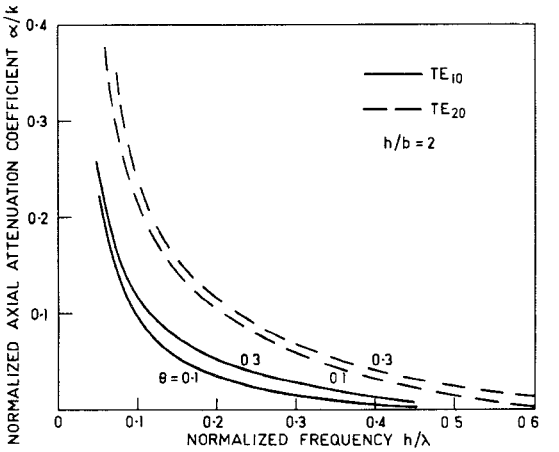

Fig. 3. Normalized axial attenuation characteristics (neglecting conduction loss).

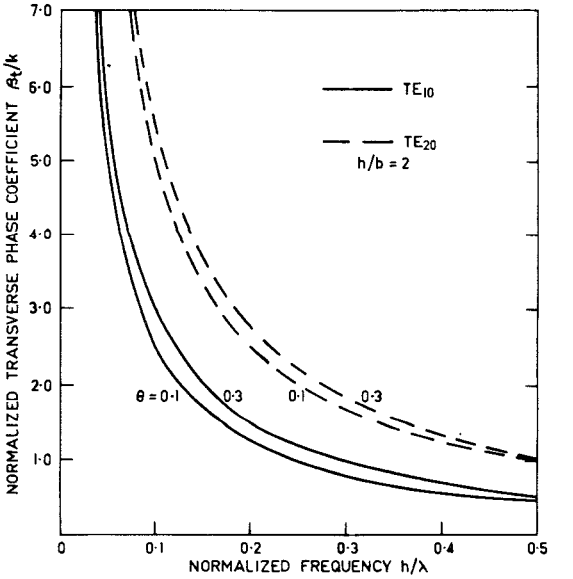

Fig. 4. Normalized transverse phase characteristics.

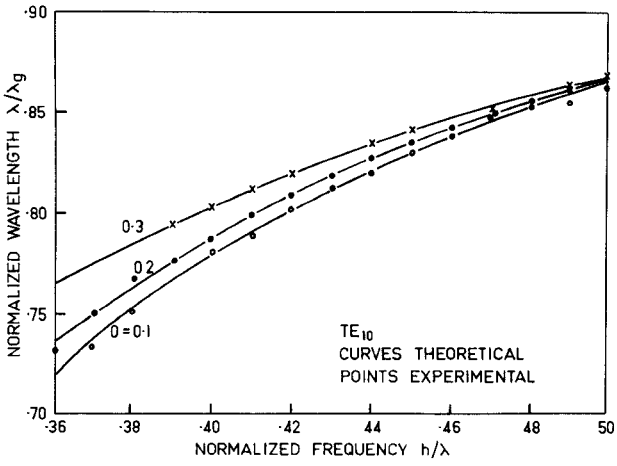

Fig. 5. Wavelength measurements.

V. Electric Field Distribution

An examination of the electric field in a transverse plane of the waveguide will give further indication of the validity of the narrow-slot and truncated-series approximations used in solving the characteristic equations. As a result of these simplifications the electric fields expressed as truncated forms of equations A_2, A_5 will only approximately satisfy the boundary conditions across the narrow dimension of the guide which includes the slot. Fig. 6 shows the variation of the electric field along a portion of the narrow wall of the guide. For $\theta > 0.3$ the electric field is no longer negligible on the metal surface. This represents the normal maximum permissible value of θ. Fig. 7 shows the electric field across the broad dimension of the guide through the center of the slot, illustrating the perturbation of the field due to the presence of the slots. The validity of the field matching is clearly evident at the center of the slot, particularly for $\theta < 0.3$.

VI. Power-Handling Capability

An indication of the power-handling capability of the slotted waveguide is given by finding the power flowing into the main section of the guide. From the Poynting vector for TE_{mn} waves

$$P = \frac{1}{2}\mathrm{Re}\int_{x=-h}^{h}\int_{y=-b}^{b} -E_{y1}H_{x1}^{*}\,dy\,dx \qquad (16)$$

where the transverse field components are found from (11). Carrying out the appropriate manipulation yields

$$P = \frac{\omega\mu b h \gamma^{*} p_n p_n^{*} A_0 A_0^{*}}{2(k_c k_c^{*})^2} \sum_{n=0}^{\infty} \Gamma_n \frac{k_c \sin n\pi\theta}{p_n n\pi\theta} \Gamma_n \left[\frac{k_c \sin n\pi\theta}{p_n n\pi\theta}\right]^{*} \times \left[\frac{\sin(p_n h - p_n^{*} h)}{(p_n h - p_n^{*} h)} + (-1)^{m+1}\frac{\sin(p_n h + p_n^{*} h)}{(p_n h + p_n^{*} h)}\right] \qquad (17)$$

where

$$\Gamma_n = \begin{cases} \dfrac{\cos k_c h}{\cos p_n h}, & m \text{ odd integer} \\ \dfrac{\sin k_c h}{\sin p_n h}, & m \text{ even integer} \end{cases} \qquad (18)$$

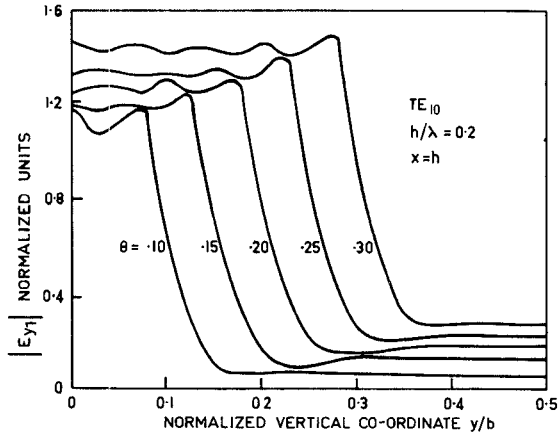

Fig. 6. Electric field strength across the slot.

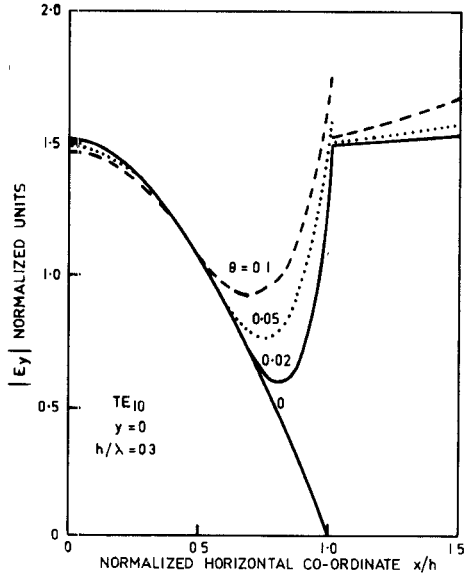

Fig. 7. Electric field strength across the waveguide.

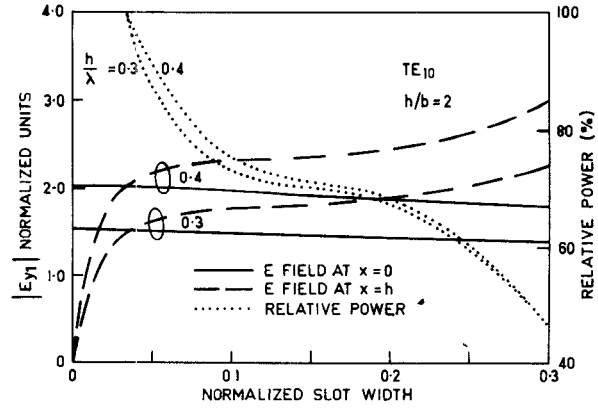

Fig. 8. Electric field strength and relative power-handling capability of slotted waveguide.

Equation (17) can be used to determine the amplitude factor A_0 for constant power input. This enables the evaluation of the electric field strength at any position in guide, particularly that at which maximum electric field occurs. Fig. 8 shows the variation in electric field strength at the center of the broad wall and at the center of the slot as a function of slot width and for two frequencies above

normal cutoff of the TE_{10} mode. Except for extremely narrow slot widths ($\theta < 0.03$), the maximum electric field occurs in the center of the slot, rather than at the center of the broad wall. Also, the field strength in the slot increases gradually with slot width. This indicates that the slotted guide is not capable of transferring as much power as the closed guide. The power-handling capability of the former also is shown in Fig. 8 as a percentage of that of the closed guide of the same dimensions. As the slot width increases, the power-handling capability decreases rapidly, with only slight improvement with increasing frequency.

VII. Conclusions

A quasi-static solution has been presented for the determination of the axial and transverse propagation coefficients of the TE leaky waves in a rectangular waveguide containing long nonresonant slots feeding parallel-plate lines in the transverse direction. The axial propagation characteristics indicate that the slots cause little change to the propagation characteristics of the closed waveguide if the slots are very thin, or if the operating frequency is far above the normal mode cutoff. A simultaneous reduction in leakage also occurs under these conditions. A normalized slot width of $\theta \approx 0.3$ represents a maximum value under which the approximate solution is valid.

Propagation also may occur below the normal mode cutoff. The axial field becomes insignificant, and the field approaches that of a TEM configuration.

The introduction of slots in the walls reduces the power-handling capability of the guide due to the increased field strength across the slots, with slight improvement occuring if the frequency is increased.

VIII. Appendix

Exact TE Wave Representation

The complete field for TE_{mn} waves with even values of m satisfying Maxwell's equations is

$$H_{z1} = \sum_{n=-\infty}^{\infty} A_n \cos p_n x \exp\left(\frac{jn\pi y}{b}\right) \tag{A1}$$

$$E_{y1} = \frac{-j\omega\mu}{k_c^2} \sum_{n=-\infty}^{\infty} A_n p_n \sin p_n x \exp\left(\frac{jn\pi y}{b}\right) \tag{A2}$$

$$E_{x1} = \frac{-j\omega\mu}{k_c^2} \sum_{n=-\infty}^{\infty} A_n \cos p_n x \frac{jn\pi}{b} \exp\left(\frac{jn\pi y}{b}\right) \tag{A3}$$

$$H_{z2} = \sum_{r=0}^{\infty} B_r \exp(jq_r x) \cos\frac{r\pi(y+d)}{2d} \tag{A4}$$

$$E_{y2} = \frac{j\omega\mu}{k_c^2} \sum_{r=0}^{\infty} B_r jq_r \exp(jq_r x) \cos\frac{r\pi(y+d)}{2d} \tag{A5}$$

$$E_{x2} = \frac{-j\omega\mu}{k_c^2} \sum_{r=0}^{\infty} B_r \exp(jq_r x) \frac{r\pi}{2d} \sin\frac{r\pi(y+d)}{2d} \tag{A6}$$

$$H_x = \frac{\gamma}{\omega\mu} E_y \qquad H_y = \frac{\gamma}{-\omega\mu} E_x \tag{A7}$$

where

$$k_c^2 = k^2 - \gamma^2. \tag{A8}$$

The condition of vanishing E_x at $y = \pm d$ is automatically satisfied and the condition of vanishing E_x at $y = \pm b$ is ensured by the constraint $A_n = A_{-n}$.

The characteristic equation is found by matching tangential fields at $x = h$ and using the Fourier method to obtain expressions for the coefficients. Matching E_y yields

$$\sum_{n=-\infty}^{\infty} A_n p_n \sin p_n h \int_{y=-b}^{b} \exp\left(\frac{jn\pi y}{b}\right) \exp\left(\frac{-jm\pi y}{b}\right) dy = \sum_{r=0}^{\infty} B_r jq_r \exp(jq_r h) \int_{y-d}^{d} \cos\frac{r\pi(y+d)}{2d} dy \cdot \exp\left(\frac{-jm\pi y}{b}\right) dy. \tag{A9}$$

The integral on the left-hand side is nonzero only when $n = m$, i.e.,

$$A_m = \frac{-j}{p_m \sin p_m h} \sum_{r=0}^{\infty} m\theta^2 \frac{B_r q_r \exp(jq_r h)}{\pi\left(m\theta + \frac{r}{2}\right)\left(m\theta - \frac{r}{3}\right)} \cdot \exp\left(\frac{jr\pi}{2}\right) \sin\pi\left(m\theta - \frac{r}{2}\right). \tag{A10}$$

Matching H_z at $x = h$ and integrating as before yields

$$B_s = \exp(-jq_s h) \sum_{n=-\infty}^{\infty} 2n\theta \frac{A_n \cos p_n h}{\pi\left(n\theta + \frac{s}{2}\right)\left(n\theta - \frac{s}{2}\right)} \cdot \exp\left(\frac{-js\pi}{2}\right) \sin\pi\left(n\theta - \frac{s}{2}\right). \tag{A11}$$

Substituting (A11) into (A10) and carrying out some simplification while maintaining consistency in the integer subscripts yields (6) given in the text. Making use of the condition of continuity of the H_y fields as $x = \pm h$ leads to a redundant equation since the H_y component is automatically accounted for by matching E_y and H_z. Using $\sin p_n x$ in (A1) and following a similar procedure yields (9) which is the equation of TE_{mn} waves for odd values of m.

Acknowledgment

The authors gratefully acknowledge the helpful discussions offered by Dr. S. Kashyap.

References

[1] E. C. Okress, *Microwave Power Engineering*, vol. 2. New York: Academic Press, 1968, pp. 126–144, 176–188.

[2] P. Bhartia, "Evaluation of parameters for the E plane applicators," *Proc. Inst. Elec. Eng.*, vol. 122, pp. 267–269, Mar. 1975.

[3] R. J. Stegun and R. H. Reed, "Arrays of closely spaced nonresonant slots," *IRE Trans. Antennas Propagat.*, vol. AP-2, pp. 109–113, Mar. 1954.

[4] V. H. Rumsey, "Traveling wave slot antennas," *J. Appl. Phys.*, vol. 24, pp. 1358–1365, Nov. 1953.

[5] L. O. Goldstone and A. A. Oliner, "Leaky-wave antennas I: Rectangular waveguides," *IRE Trans. Antennas Propagat.*, vol. AP-7, pp. 307–319, Oct. 1959.

[6] G. K. Snurnikova, "Propagation of electromagnetic waves in a grooved waveguide," *Radio Eng. Electron. Phys.*, vol. 15, pp. 509–511, 1970.